Proceedings of 14th International Conference on Mesomechanics, Budapest, Hungary, Sept. 25-28. 2012

Prediction of fatigue crack propagation in aluminum alloy with local yield strength gradient at the crack path

A.T. Kermanidis[a], A. Tzamtzis[b]

[a]*Laboratory of Mechanics and Strength of Materials, Department of Mechanical Engineering, e-mail: akermanidis@mie.uth.gr*
[b]*Laboratory of Mechanics and Strength of Materials, Department of Mechanical Engineering, e-mail: atzam@uth.gr*

Abstract

The effect of yield strength gradient on fatigue crack propagation of aluminum alloy 2024-T3 has been experimentally and analytically investigated. A special heat treatment process was utilized to achieve over aging material conditions resulting in a controlled, local yield strength variation. Fatigue crack growth tests were conducted on reference material and over aged material with local strength gradient. The results have shown that controlled over aging conditions resulting in local strength gradients influence fatigue crack propagation behavior. The experimental results were compared with analytical predictions using the LTSM-F fatigue crack growth code. The crack growth rate equation in the code was appropriately revised to account for the yield strength gradient at the crack tip. The results indicated that in most cases the code was able to describe successfully the experimentally obtained crack growth trends.

Keywords: fatigue; yield strength gradient; crack propagation; crack path

1. Introduction

Local strength variations in metallic structures are common at welded joints, which include material inhomogeneities. Weld regions are characterised by the simultaneous presence of material zones with varying microstructure such as base material, heat affected zone and weld pool. Material overaging caused by the welding process leads to local degradation of strength in the form of gradients within these zones. The variations of yield strength in ductile aluminium alloys are expected to influence stage II fatigue crack propagation due to associated changes in the material's ability to cyclically deform or strain harden at the crack tip [1-6].

Strength gradients and their influence on fatigue crack propagation in aluminium alloys have received only limited attention in literature. An early study performed by Reifsnider et al. [7] reported deviations of fatigue crack propagation rates in aluminum alloys of 6xxx and 7xxx series including strength gradient with regard to the reference material. In the case of 2xxx aluminum alloys however relevant experimental data are missing. Furthermore, crack propagation models usually do not take into account the effect of strength gradients in crack growth analyses. The development of models which can take into account variations of material strength at the crack path can facilitate in special cases, as in weld regions, a more accurate prediction of crack growth.

In the present study, the effect of yield strength profile on fatigue crack propagation (FCP) of 2024 aluminum alloy was studied experimentally. Strength profiles were inserted in the material by means of a controlled heat treatment process. An analytical model was used to assess the influence of strength profile on material's fatigue crack growth behavior.

2. Heat treatment

Clad 2024 aluminum alloy has been used in T3 condition, which includes heat treatment, control stretching and natural aging. The alloy was received in sheet form of 3.2 mm thickness. The clad surface thickness was 0.125 mm.

Controlled heat treatment process was used to achieve over aging conditions HT1 and HT2 in the material. HT1 corresponds to aging for 15 hours at constant temperature to achieve uniform yield strength reduction with regard to T3 condition. The temperatures used were 250 °C and 300 °C for 15 hours. HT2 treatment included exposure of the samples to a temperature gradient between two temperature boundaries from 300 to 200 °C to achieve a gradual decrease of micro-hardness between the two boundaries. Typical results of hardness profiles in the material after HT2 are shown in Fig. 1.

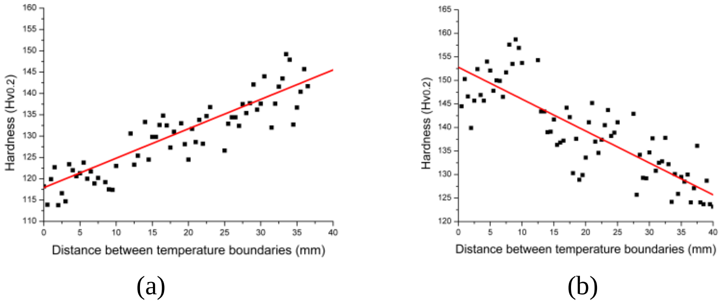

Figure 1. Typical hardness profiles of specimens after HT2 treatment; (a) linear hardness increase with distance (HT2 G1); (b) linear hardness decrease with distance (HT2 G6)

Table 1. Hardness and mechanical properties for reference and HT1 treated material

	Hardness Vickers	Yield strength (σ_y)
Reference 2024 T3	153 HV	366-377 MPa
HT1 (250 °C – 15h)	115-120 HV	257-263 MPa
HT1 (300 °C – 15h)	76-81 HV	145-158 MPa

Table 2. Mathematical expression of linear fit for different strength gradients

Heat treatment	Least square fit
HT2 G1	0.69x+117,92
HT2 G4	0.59x+122.52
HT2 G5	0.53x+125.34
HT2 G2	-0.54x+152,97
HT2 G3	-0.65x+147,30
HT2 G6	-0.68x+152,79

In Table 1 hardness and mechanical properties for reference and HT1 treated material are given. The relation between hardness and yield strength values was obtained empirically based on the values in Table 1. in the form $\sigma_y = 3 \cdot HV - 90$ and is used in section 4 of this paper. The least square fit method has been applied on the hardness measurements to determine the mathematical expression describing variation of yield strength with distance (strength gradient). The results for the cases G1-G6 of strength gradients examined are given in Table 2.

3. Experimental

3.1. Fracture Toughness tests

Fracture toughness tests were performed on C(T) specimens shown in Fig. 2c in accordance with ASTM E561-98. The difference of fracture toughness specimens compared to the specimens used in FCP tests was the initial notch length (here 21mm). The maximum mode I stress intensity factor (K_{max}) was determined as the maximum value that complies with LEFM conditions in the test. The experimental results of K_{max} are displayed in Figs 2a and 2b for T3 and HT1 treatment.

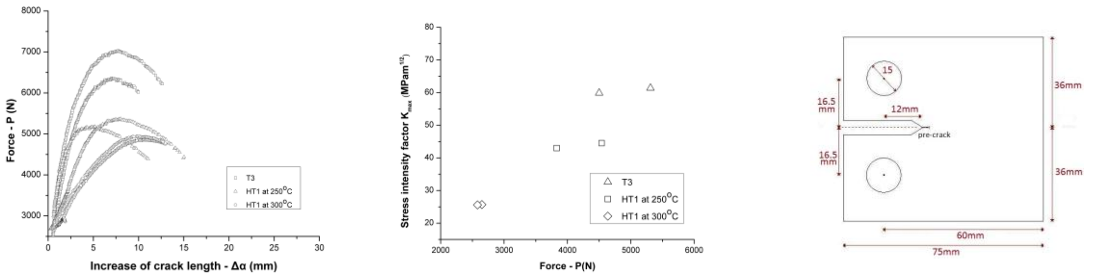

(a) (b) (c)

Figure 2. Fracture toughness measurements for T3 and HT1 materials; (a) Force – Crack length diagrams; (b) K_{max} values; (c) C(T) specimen configuration

3.2. Fatigue crack growth tests

Fatigue crack propagation tests were conducted using compact tension C(T) specimens in accordance with ASTM E647-00. The tests were carried out on a 100KN servo-hydraulic fatigue machine at room temperature with a constant stress ratio of R=0.1. The maximum stress was σ_{max}= 10MPa and the frequency 5Hz. Crack length measurements were made using a crack opening displacement (COD) gauge and subsequent data evaluation by implementation of the compliance method. The crack growth characteristics were examined in T3, HT1 and HT2 conditions. The C(T) specimens with HT2 treatment were appropriately machined so that the axis at the notch tip perpendicular to the notch plane coincides with a boundary of strength gradient (Fig. 4a).

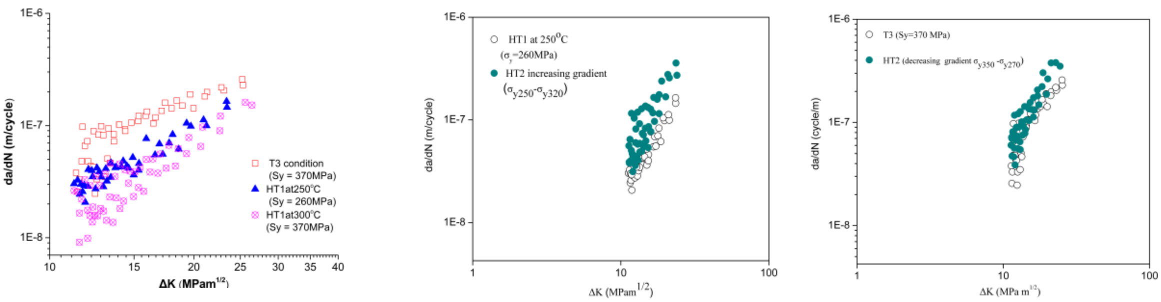

(a) (b) (c)

Figure 3. (a) comparison of FCP rates between reference material and HT1 treatment; (b) comparison of FCP rates between HT1 (250) and HT2 treatment (increasing); (c) comparison of FCP rates between reference (T3) material and HT2 (decreasing)

In Figs. 3a, b, c the fatigue crack growth results of 2024 material in T3 state with HT1 and HT2 heat treatments are compared. Crack growth rates were measured at an intermediate ΔK region ranging from 11 to 25 $MPam^{1/2}$.

The results indicate a pronounced effect of HT1 treatment on FCG rates with regard to T3 material (Fig. 3a). Crack growth resistance is enhanced in HT1 specimens compared to T3 and increases further with the over aging temperature of HT1. In the case of HT2 treatment an opposite effect is observed. The strength gradient degrades FCP performance as shown in Fig3. The reference material behavior, in this case is the state of the material prior to the crack tip entering the strength profile. Crack growth rates of HT2 specimens were higher with regard to the reference behaviour in the whole ΔK range examined. Several factors may play a role in the observed behavior. Over aging conditions achieved with HT1 treatment in 250 °C and 300 °C introduce an increasing strain hardening rate of the material with increasing over aging temperature. Generally this is associated with blockage of dislocations around non coherent strengthening precipitates and formation of dislocation loops around strengthening particles. A thorough investigation on the microstructural influences on the observed crack propagation behavior is an ongoing investigation and exceeds the scope of the present work. Nevertheless, the change in strain hardening behavior may influence fatigue crack propagation. Also, the reduced yield strength may contribute to higher crack tip plasticity and possible increased closure of crack surfaces. This requires verification with ΔK_{eff} experiments. In the case of yield strength gradient (HT2 state) the justification for increased crack growth rates is more complex and requires further investigation supported by ΔK_{eff} experiments, fractography and electronic microscopy for better understanding of the underlying mechanisms that influence crack growth.

4. Crack growth calculation

The LTSM-F crack growth model [8] has been implemented to account for the strength gradient effect at the crack tip area. In the model constant stress amplitude conditions have been considered and cyclic plasticity is incorporated in terms of reversed plastic zone ωs (Fig. 4a).The material ahead of the crack tip, where the strength gradient applies is predominantly under elastic strain conditions. In the model the crack growth equation for constant amplitude stress is given in the form:

$$\frac{d\alpha}{dN} = \left(\frac{\sqrt{A}}{\sqrt{2}K_{cr}}\right)^{2/m} \left(\frac{\pi}{32\sigma_y{}^2}\right)^{1-\frac{\beta-1}{m}} \Delta K^{2(1-\frac{\beta-2}{m})} \tag{1}$$

Crack length with the number of cycles is numerically calculated with the expression:

$$\alpha = \alpha_i + \sum_{i=1}^{k} \left(\frac{d\alpha}{dN}\right) \tag{2}$$

The material constants A and β in Eq (1) are fitted experimentally as described in [8]. The calculated values for the reference T3 material are A=7,823·10^{-5} and β=1,973. The maximum mode I stress intensity factor that corresponds to the C(T) specimen (K_{cr} in Eq 1) was taken from Fig. 2b. K_{max}=60 $MPam^{1/2}$. In order to include the strength gradient effect of fatigue crack growth calculation the value σ_y in Eq (1) has been replaced with the empirical relation between yield strength and hardness $\sigma_y = 3 \cdot HV - 90$ and the use of the expression $HV = K \cdot x + \zeta$ (see Table 2). HV is the Vickers hardness value inside the gradient at a distance x (Fig 3b), x is the distance from the notch tip and ζ is the hardness value at the notch tip of the C(T) specimen for each case.

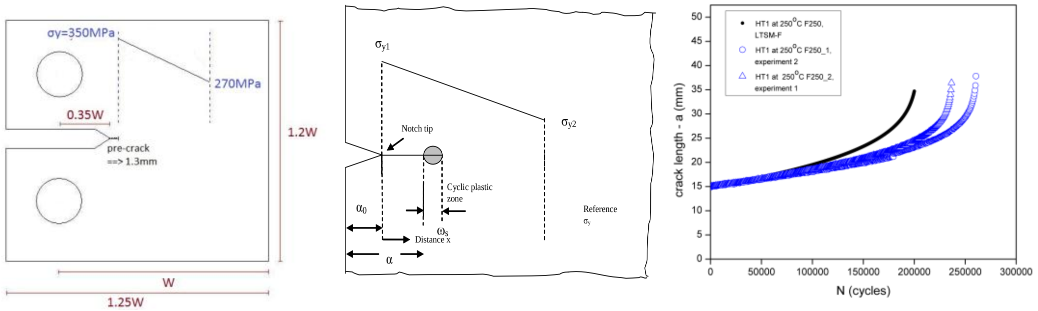

(a) *(b)* *(c)*

Fig 4 (a) Strength gradient at notch tip; (b) FCP inside strength gradient; (c) a-N curves for HT1(250)

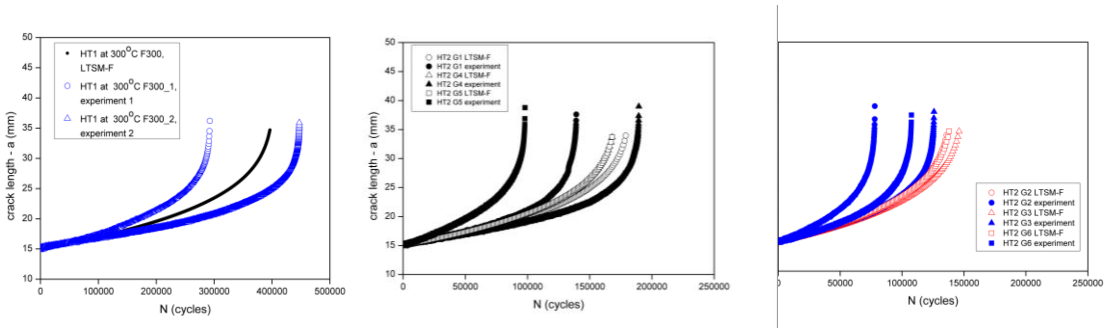

(a) *(b)* *(c)*

Fig 5 (a) a-N curves for HT1(300); (b) *a-N* curves for HT2(increasing); (c) *a-N* curves for HT2(decreasing)

The results using the modified Eq (1) are compared against the experimental results in Figs 4c and 5a, 5b, 5c. The calculated crack growth follows the experimental trends with a slight underestimation or overestimation of fatigue life depending on the case examined. Definitive conclusions cannot be drawn to the existent scatter of experimental data but in the case of HT1 (250) there is an underestimation of 20% in fatigue life, in HT1 (300)~~,~~; calculation agrees well with experiment, while in HT2 treatment there is some overestimation in the calculated values. It should be noted that the analytical results are predictions based on the strength values of the material using the crack growth constants *A*, *β* of reference (T3) material.

5. Conclusions

The effect of strength gradient introduced by specific heat treatments on FCP of 2024 alloy was experimentally and analytically investigated. The experimental findings showed that HT1 treatment enhances the fatigue crack propagation behavior compared to the reference material. HT2 treatment (strength gradient) results in increased crack growth rates compared to T3 state. The strength gradients obtained by heat treatment were introduced in the LTSM-F crack growth rate equation. The analytical predictions were able to follow the fatigue crack propagation trends obtained in the experiments with small over or underestimation of fatigue lives depending on the treatment.

Acknowledgments

This research has been co-financed by the European Union (European Social Fund - ESF) and Greek national funds through the Operational Program "Education and Lifelong Learning" of the National Strategic Reference Framework (NSRF) – Research Funding Program: Heracleitus II. Investing in knowledge society through the European Social Fund.

References

[1] Putatunda S K, Influence of Material Strength Level on Fatigue Crack Closure. Eng. Fract. Mech. 1988;50 (5): 627-39.

[2] Raghuvir K, Garg S B L. Effect of Yield Stress and Stress Ratio on Fatigue Crack Closure in 6063-T6 Aluminium Alloy. Int. J. Pres. lies. & Piping 1989;38: 293-307.

[3] Jones R E..Fatigue crack growth retardation after a single-cycle peak overload in Ti–6Al–4V titanium alloy. Eng Fract Mech; 1973;5:585–604.

[4] Kassim S, Al-Rubaie A. Emerson K L, Barroso A, Leonardo B, Godefroid B. Fatigue crack growth analysis of pre-strained 7475–T7351 aluminum alloy. International Journal of Fatigue 2006;28: 934–42

[5] Schijve J. The effect of pre-strain on fatigue crack growth and crack closure. Eng Fract Mech 1976;8:575-81.

[6] Telesman J, Antolovich S D. A study of spectrum fatigue crack propagation in two aluminium alloys-II Influence of microstructures. Eng. Fract. Mech. 1986;24 No 3:463-77

[7] Reifsnider K, Kahl M. Effect of Local Yield Strength Gradients on Fatigue Crack Propagation. Int. J. Mech. Sci. 1974;16:105-119

[8] Kermanidis A T, Pantelakis Sp G. Fatigue Crack Growth Analysis of 2024 T3 Aluminum Specimens Under Aircraft Service Spectra. Fat. and Fract.of Eng. Mat. and Struct., 2001;24:699-710.